

# In Vitro Analysis of the *Escherichia coli* AmtB-GlnK Complex Reveals a Stoichiometric Interaction and Sensitivity to ATP and 2-Oxoglutarate<sup>\*[5]</sup>

Received for publication, March 16, 2006, and in revised form, July 14, 2006. Published, JBC Papers in Press, July 24, 2006, DOI 10.1074/jbc.M602477200

Anne Durand and Mike Merrick<sup>1</sup>

From the Department of Molecular Microbiology, John Innes Centre, Norwich NR4 7UH, United Kingdom

In *Escherichia coli*, the ammonia channel AmtB and the P<sub>II</sub> signal transduction protein GlnK constitute an ammonium sensory system that effectively couples the intracellular nitrogen regulation system to external changes in ammonium availability. Binding of GlnK to AmtB apparently inactivates the channel, thereby controlling ammonium influx in response to the intracellular nitrogen status. We designed an N-terminally histidine-tagged version of AmtB with a native C-terminal region in order to purify the AmtB-GlnK complex. Purification revealed a stable and direct interaction between AmtB and GlnK, thereby showing for the first time that stability of the complex does not require other proteins. The stoichiometry of the complex was determined by two independent approaches, both of which indicated a 1:1 ratio of AmtB to GlnK. We also showed by mass spectrometry that only the fully deuridylylated form of GlnK co-purifies with AmtB. The purified complex allowed *in vitro* studies of dissociation and association of AmtB and GlnK. The interaction of GlnK with AmtB is dependent on ATP and is also sensitive to 2-oxoglutarate. Our *in vitro* data suggest that *in vivo* association and dissociation of the complex might not only be dependent on the uridylylation status of GlnK but may also be influenced by intracellular pools of ATP and 2-oxoglutarate.

Under nitrogen-limiting conditions, the uptake of ammonium into the cells of many organisms is mediated by a class of ubiquitous membrane proteins, designated Amt (ammonium transporter) proteins (1). They are present in bacteria, archaea, fungi, and plants, whereas in animals, from nematodes to humans, they are represented by the closely related Rh (Rhesus) proteins. The most studied Amt protein is *Escherichia coli* AmtB, which is a stable homotrimer in the cytoplasmic membrane and retains this structure when purified and reconstituted in two-dimensional crystals (2, 3). The first 22 residues of *E. coli* AmtB encode a signal peptide (1, 4) that is cleaved from the preprotein upon membrane insertion so that the mature

protein has an N<sub>out</sub> and C<sub>in</sub> topology (1, 5, 6). The x-ray crystal structures of *E. coli* AmtB and *Archaeoglobus fulgidus* Amt-1 have been solved and are very similar (5–7). They are both trimers in which each subunit is formed by 11 transmembrane helices (TMH).<sup>2</sup> The structure has a pseudo-2-fold symmetry with the 2-fold axis in the middle plane of the membrane, relating helices TMH1 to TMH5 and TMH6 to TMH10, with TMH11 across the lipid-accessible face of each monomer. In the *E. coli* AmtB structures, the last 20 amino acids, which are predicted to constitute a cytoplasmic region, are disordered. However, the equivalent region of *A. fulgidus* Amt-1 was resolved, and it folds into two short  $\alpha$ -helices (7). The Amt structures revealed that transport occurs through a narrow mainly hydrophobic pore located at the center of each monomer. Computer simulations and structural and energetic data, together with *in vivo* and *in vitro* assays, indicate that ammonium is the substrate recognized by AmtB but that ammonia is the translocated species (5, 6, 8–10). Therefore, the Amt proteins have been described as ammonia gas channels, as previously proposed (11).

Almost all bacteria and archaea encode at least one Amt protein, and, with very few exceptions, the structural gene (*amtB*) is genetically linked to a second gene (*glnK*) that encodes a small cytosolic signal transduction protein (12). GlnK is a member of the P<sub>II</sub> protein family, of which *E. coli* encodes two members, GlnK and GlnB. These proteins act as sensors of the cellular nitrogen status in prokaryotes, and they have also been identified in plants (13). In a variety of organisms, P<sub>II</sub> proteins have been shown to regulate the activities of other proteins by protein-protein interaction (13–15). P<sub>II</sub> targets are diverse and have different functions (including enzymes and transcription factors), different structures, and different cellular localizations (cytosol and membrane). Among the P<sub>II</sub> crystal structures determined so far, those of *E. coli* GlnB and GlnK have both been solved, and they are very similar (16–18). Both proteins are homotrimers of 112 amino acids that form a compact barrel of ~50 Å in diameter and 30 Å high. Each monomer consists of a four-stranded  $\beta$ -sheet that packs against two helices. A relatively unstructured loop (the T-loop), connecting strands  $\beta$ 2 and  $\beta$ 3, protrudes from the upper surface. Two other notable loops are present in the structure: the B-loop connecting helix  $\alpha$ 2 and strand  $\beta$ 4, and the C-loop regrouping the C-terminal residues. A lateral cleft between each subunit is formed

\* This work was supported by the Biotechnology and Biological Sciences Research Council (BBSRC) (United Kingdom). The Joint IFR-JIC Proteomics Facility is funded in part by BBSRC JREI Grants JRE10832, JE412701, and JE412631 and grants from Syngenta and Unilever. The costs of publication of this article were defrayed in part by the payment of page charges. This article must therefore be hereby marked "advertisement" in accordance with 18 U.S.C. Section 1734 solely to indicate this fact.

[5] The on-line version of this article (available at <http://www.jbc.org>) contains Tables S1 and S2.

<sup>1</sup> To whom correspondence should be addressed: Dept. of Molecular Microbiology, John Innes Centre, Norwich NR4 7UH, United Kingdom. Tel.: 44-1603-450749; Fax: 44-1603-450778; E-mail: mike.merrick@bbsrc.ac.uk.

<sup>2</sup> The abbreviations used are: TMH, transmembrane helix; LDAO, *n*-dodecyl-*N,N*-dimethylamine-*N*-oxide; 2-OG, 2-oxoglutarate; WT, wild-type.

Supplemental Material can be found at:  
<http://www.jbc.org/cgi/content/full/M602477200/DC1>



## *E. coli* AmtB-GlnK Complex

Sall fragment of pSTUART1. pAD4 was derived by cloning the NdeI/BamHI fragment of pESV2 (31) into NdeI/BamHI-cut pAD2. To construct pAD5 (WT GlnK) and pAD6 (Y51F GlnK), the BstXI/BamHI PCR fragment of pAD2 was amplified using the oligonucleotides 5'-ACGGCGTTTGTGGCATTGTCGGC-3' (forward) and 5'-CCGGATCCTTACGCGTTATAGGCATTCTCGC-3' (reverse; BamHI site underlined). The PCR product was inserted into the BstXI/BglII sites of pAJ1002 (31) and pAJ1023, respectively. pAJ1023 was derived from pAJ1004 (31) by reversing an unexpected point mutation found in pAJ1004 that causes a Phe-55 to Ser-55 substitution. The QuikChange<sup>TM</sup> multisite-directed mutagenesis kit (Stratagene) was used with the oligonucleotide 5'-CGGAATTCAGCGTCAATTTCTGCGCAA-3' so that pAJ1023 now encodes GlnK Y51F and not Y51F,F55S.

**Protein Purification**—To purify the AmtB-GlnK complex, we used GT1000 as the host strain (32) to avoid any contamination with the host-derived AmtB. GT1000(pAD2) cells were grown aerobically overnight at 30 °C in M9Gln containing 15 μg/ml chloramphenicol. Before harvesting the cells, a 30 mM ammonium chloride shock of 15 min was performed. The cell pellet was resuspended in 50 mM Tris-HCl, pH 8.0, 100 mM NaCl and lysed by two passages through a French pressure cell, 15,000 psi at 4 °C. The extract was clarified by centrifugation for 30 min at 43,000 × *g* in a SS-34 Sorvall rotor at 4 °C. The supernatant (whole cell extract) was centrifuged at 210,000 × *g* in a Kontron TFT 65-13 rotor for 1 h at 4 °C. The membrane pellet was resuspended to 1.5 mg/ml protein in 50 mM Tris-HCl, pH 8.0, 100 mM NaCl, 10% (v/v) glycerol and frozen overnight at -80 °C. The membranes were thawed on ice and solubilized with 2% (w/v) *n*-dodecyl-*N,N*-dimethylamine-*N*-oxide or LDAO (Anatrace) at 4 °C for 2 h. The complex was also purified using the nonionic detergents *n*-octyl-β-*D*-glucopyranoside and *n*-dodecyl-β-*D*-maltopyranoside, but the complete characterization of the complex utilized material solubilized in LDAO.

The solubilized membranes were centrifuged at 210,000 × *g* for 1 h. The resultant supernatant was applied to a Hi-Trap chelating column (Amersham Biosciences) prepared by saturation with 100 mM NiCl<sub>2</sub> and equilibrated with 50 mM Tris-HCl, pH 8.0, 100 mM NaCl, 10% (v/v) glycerol, 0.05% (w/v) LDAO (buffer A) containing 5 mM imidazole at 1 ml min<sup>-1</sup>. The elution was performed after a two-step gradient with buffer A containing 80 mM imidazole and 300 mM imidazole. For Superose 12 10/300 GL (Amersham Biosciences) size exclusion chromatography, the AmtB-GlnK fraction eluting from the Ni<sup>2+</sup> column was concentrated with a 50,000 cut-off Centricon filter (Millipore). A 500-μl sample was then loaded onto the S12 column preequilibrated with buffer A and run at 0.2 ml min<sup>-1</sup>.

APAVAH<sub>6</sub>-AmtB was purified from GT1000(pAD4) as described for the complex purification, except that no ammonium shock was performed before harvesting the cells, and the protein was eluted from the Ni<sup>2+</sup> column after a step gradient with buffer A containing 300 mM imidazole. APAVAH<sub>6</sub>-AmtB was quantified by amino acid composition analysis and used as standard for titration gels. AmtB-DH<sub>6</sub> was purified from C43(pMM285) as described previously (2). Native *E. coli* GlnK was purified as described previously (26). It was used as a standard for titration gels and as a control for mass spectrometry analysis.

**Analytical Size Exclusion Chromatography**—The molecular mass markers (100 μl) and samples (usually 500 μl) were eluted at room temperature in 50 mM Tris-HCl, pH 8.0, 100 or 250 mM NaCl, 10% (w/v) glycerol, 0.05% (w/v) LDAO at a flow rate of 0.2 ml min<sup>-1</sup>, on a Superose 12 10/300 GL column. The molecular mass standards (Sigma and Amersham Biosciences) used for the calibration were as follows: β-amylase, 200 kDa; aldolase, 158 kDa; bovine serum albumin, 67 kDa; carbonic anhydrase, 29 kDa; cytochrome *c*, 12.4 kDa.

**Effect of Small Effectors on the AmtB-GlnK Complex**—To study the influence of small effectors on stability of the AmtB-GlnK complex, we immobilized the purified complex (100 μg) on HIS-Select spin columns (Sigma) previously equilibrated with buffer A containing 5 mM imidazole. The flow-through was collected, and unbound proteins were removed by three washes with the same buffer. Three additional washes were carried out in buffer A with 5 mM imidazole in the absence or presence of effectors: 0.1, 1, or 2 mM 2-OG; 3.5 mM ATP; 5 mM MgCl<sub>2</sub>. As a control, the immobilized complex was dissociated by treating with 600 mM NaCl. For each condition tested, a single column was used. Elution of APAVAH<sub>6</sub>-AmtB or APAVAH<sub>6</sub>-AmtB-GlnK complex was performed by the addition of buffer A containing 500 mM imidazole. The washed fractions, collected after applying effectors, and the eluted fraction were loaded on 12.5% SDS-polyacrylamide gels and stained with Coomassie Blue.

For *in vitro* reconstitution of the complex, AmtB and GlnK were obtained by purifying the complex, as described previously, and then dissociating the proteins from a Ni<sup>2+</sup> column in the presence of 600 mM NaCl. In those conditions, GlnK was in the unbound fraction, and AmtB was subsequently eluted using increasing concentrations of imidazole. The two proteins were then loaded independently on a size exclusion chromatography column (Superose 12 10/300) in buffer A. Pure AmtB and GlnK were preincubated in a molar ratio of 1:2 in buffer A with 5 mM imidazole in the absence or presence of effectors (0.1, 1, or 2 mM 2-OG; 3.5 mM ATP; 5 mM MgCl<sub>2</sub>) for 15 min at 30 °C. The mixture was then loaded onto a HIS-Select spin column (Sigma) previously equilibrated with 5 mM imidazole in buffer A containing the same effectors as in the initial reaction mixture. For each condition tested, one column was used. The flow-through was collected, and unbound proteins were removed after three washes with the same buffer containing the effectors present in the reaction mixture. Elution was performed with 500 mM imidazole in buffer A, and the eluted fractions were analyzed for the presence of AmtB and GlnK by Western blotting.

**Protein Quantification**—Pure proteins, cell extracts, and subcellular fractions were assayed with Bradford reagent (Sigma) using bovine serum albumin (Sigma) as a standard. Concentrations of proteins used as standards for Coomassie-stained gels were determined by quantitative amino acid composition at the Protein and Nucleic Acid Chemistry (PNAC) Facility in Cambridge.

**Amino Acid Composition**—The amino acid compositions of the purified AmtB-GlnK complex, of GlnK, and of AmtB were determined after a 22-h acid hydrolysis at 115 °C, according to the method described previously (37). The free amino acids

were separated on an ion exchange resin (sodium system) eluting with a series of buffers over the pH range 3.20–6.45 on an amino acid analyzer (Amersham Biosciences Alpha Plus Series II). Peak detection was achieved by mixing the eluate with ninhydrin at 135 °C and measuring the absorbance (at 570 and 440 nm). Quantitation was performed using Chromeleon software and calibration curves for each amino acid of interest.

**Quantitative Coomassie Gels**—Samples were subjected to SDS-PAGE (10 and 15% for AmtB and GlnK analysis, respectively) and stained with Coomassie Blue. The intensity of bands was converted to a protein concentration by using a calibration curve of pure protein present on each gel. Each Coomassie-stained gel was loaded with seven different dilutions of a protein standard (AmtB (27.6, 23.6, 19.7, 15.8, 11.8, 7.9, and 3.9 pmol of trimer) and GlnK (163.2, 122.3, 81.6, 40.8, 20.4, 10.2, and 5 pmol of monomer)) and six different dilutions of the pure complex (5, 4, 3, 2, 1, and 0.5 μg). Accurate concentrations of AmtB and GlnK used as standards were determined by amino acid composition. The signal was scanned and quantified with GeneTools software (Syngene).

**Data Analysis**—To calculate the AmtB/GlnK stoichiometry, we used a mathematical model in which we compared the values of the experimental amino acid composition of the complex with the respective amino acid compositions of AmtB and GlnK. Asparagine and glutamine are converted to aspartate and glutamate, respectively; therefore, Asx and Glx correspond to the amount of Asp + Asn and Glu + Gln, because Asn and Gln are deamidated following the acid treatment. Norleucine was used as an internal standard but is not reported.

We used the data from two different amino acid composition estimations to calculate the stoichiometry (*s*) of the AmtB-GlnK complex, with *s* representing the number of GlnK mol for 1 mol of AmtB (AmtB/*s* GlnK). The value of *s* was calculated by using the Solver tool in Microsoft Excel to minimize the mean square deviation between the calculated fractions of each amino acid in the complex and the fractions obtained with the experimental data. The calculated fraction was obtained using the following equation,

$$\frac{n_{aa}^{\text{AmtB-GlnK}}}{N^{\text{AmtB-GlnK}}} = \frac{n_{aa}^{\text{AmtB}} + (s \times n_{aa}^{\text{GlnK}})}{N^{\text{AmtB}} + (s \times N^{\text{GlnK}})} \quad (\text{Eq. 1})$$

where  $n_{aa}$  is the number of one particular amino acid in AmtB, GlnK, or AmtB-GlnK, and  $N$  is the number of all of the amino acids used for the calculation in AmtB, GlnK, or AmtB-GlnK. All of the amino acids reported in supplemental Table S1 were included in the calculation. Valine and isoleucine data were not used, because upon acidic hydrolysis, the peptide bonds of Ile-Ile, Val-Val, Ile-Val, and Val-Ile are only partially cleaved, and consequently, the values obtained for Val and Ile can be underestimated. AmtB and GlnK do not have comparable numbers of those peptide bonds; therefore, we did not consider those two residues for estimation of the stoichiometry.

**N-terminal Sequence Determination**—This was carried out using an Applied Biosystems Procise 494 Protein Sequencer to analyze the complex from a polyvinylidene fluoride membrane (PNAC, Cambridge, and Krebs Institute Sequencing and Synthesis Facility, University of Sheffield).

**Mass Spectrometry Analysis**—Free GlnK was isolated from the AmtB-GlnK complex after two chromatographic steps (Ni<sup>2+</sup> affinity followed by size exclusion chromatography) in the presence of high salt buffer. The protein was eluted from the Superose 12 10/300 GL in 50 mM Tris-HCl, pH 7.6, 250 mM NaCl, 10% (v/v) glycerol, and 1 mM EDTA. Its mass was compared with that of a purified deuridylylated form of GlnK. The intact mass of the proteins was then analyzed by mass spectrometry using sinapinic acid as matrix on an UltraFlex MALDI-TOF/TOF from Bruker (Coventry, UK) at the IFR-JIC Proteomics Facility.

**Western Blotting**—Western blotting was performed as previously described (32), and proteins were detected with either anti-*E. coli* GlnK or anti-*E. coli* AmtB (31) antibodies.

**[<sup>14</sup>C]Methylammonium Transport Assays**—Unwashed assays were performed at room temperature as described previously (9).

## RESULTS

**Characterization of an N-terminally Histidine-tagged AmtB**—To optimize and mimic the natural interaction between AmtB and GlnK, we constructed a plasmid (pAD2) to express WT GlnK and APAVAH<sub>6</sub>-AmtB under the control of the native promoter of the *glnKamtB* operon. Expression of *glnKamtB* is consequently inducible by nitrogen limitation. AmtB has a WT C terminus and an AVAH<sub>6</sub> sequence inserted in the N-terminal region, two residues downstream from the natural signal peptide cleavage site and before TMH1. Using this construct, we first checked expression of GlnK and AmtB, *in vivo* uptake of methylammonium, and the correct cellular localization of the two proteins.

Expression of GlnK and AmtB was induced by growing cells overnight in nitrogen-limited conditions. As shown on Western blots, APAVAH<sub>6</sub>-AmtB was located in the membrane and run on a 10% SDS-polyacrylamide gel at ~90 kDa and with the same mobility as AmtB-DH<sub>6</sub> that is known to run as a stable trimer on SDS-PAGE (2) (Fig. 1A). Therefore, APAVAH<sub>6</sub>-AmtB apparently also folds into a homotrimer. Furthermore, the additional residues in the N-terminal region do not dramatically affect the interaction between the subunits, because neither dimeric (~66 kDa) nor monomeric (~33 kDa) forms were observed on the Western blot. The trimeric form of an equivalent protein carrying only the histidine tag and not the AVA insertion (APH<sub>6</sub>-AmtB) was less stable on reducing SDS-PAGE when compared with APAVAH<sub>6</sub>-AmtB (data not shown).

After an ammonium shock, GlnK, expressed together with the APAVAH<sub>6</sub>-AmtB from pAD2, was sequestered efficiently to the membrane, and no GlnK was detected in the cytoplasm (Fig. 1B). By contrast, there was still some GlnK in the cytosol when using AmtB derivatives with extra residues at the C terminus of AmtB (*i.e.* AmtB-DH<sub>6</sub> (pJT6) and AmtB-DL (pJT6E)) (Fig. 1B). For all three AmtB constructs, there was no major difference in the levels of AmtB in the membrane (Fig. 1C) or in the total amounts of GlnK in the whole cell extracts (data not shown). Hence, the reduced binding of GlnK to the membrane with some AmtB variants could be due to a decreased interaction with AmtB, because of the extra residues present at its C terminus. Alternatively, the different AmtB variants could affect the intracellular nitrogen status following an ammonium

## *E. coli* AmtB-GlnK Complex

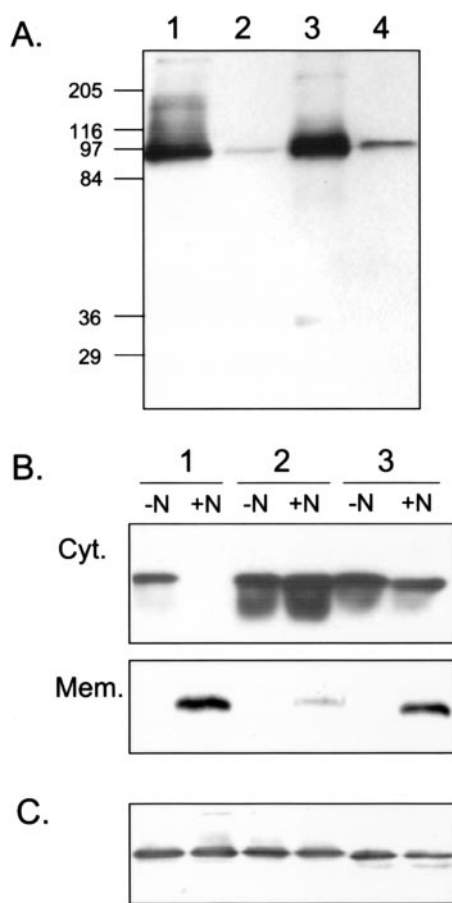


**FIGURE 1. Expression of an N-terminally histidine-tagged AmtB (APAVAH<sub>6</sub>-AmtB) and GlnK sequestration.** *A*, lanes 1–3, whole cell extracts (5  $\mu$ g), cytoplasmic (5  $\mu$ g), and membrane (0.5  $\mu$ g) fractions, respectively, prepared from GT1000(pAD2), expressing GlnK APAVAH<sub>6</sub>-AmtB, after an ammonium shock, were subjected to 10% SDS-PAGE followed by Western blotting using anti-AmtB antibodies (1:10,000). Lane 4, pure AmtB-DH<sub>6</sub> (10.5 ng) purified from C43(pMM285) and used as a control. Molecular mass marker positions (kDa) are shown on the left. *B*, 5  $\mu$ g of cytoplasmic (Cyt) and membrane (Mem) fractions prepared from GT1000(pAD2):APAVAH<sub>6</sub>-AmtB (lane 1), GT1000(pJT6):AmtB-DH<sub>6</sub> (lane 2), and GT1000(pJT6E):AmtB-DL (lane 3), before (–N) and after (+N) an ammonium shock were subjected to 15% SDS-PAGE followed by Western blotting using anti-GlnK antibodies (1:5000). *C*, membrane (5  $\mu$ g) fractions as described above (*B*) were subjected to 10% SDS-PAGE followed by Western blotting using anti-AmtB antibodies (1:10,000).

shock, thereby leading to a difference in the uridylylation status of GlnK.

Methylammonium uptake activity was assayed after growing cells overnight under nitrogen-limiting conditions. The activity of APAVAH<sub>6</sub>-AmtB co-expressed either with (pAD2) or without (pAD4) GlnK was  $82 \pm 9$  and  $100 \pm 7\%$ , respectively ( $n = 3$ ), of that of a nontagged version of AmtB encoded on pSTUART or AmtB-DL encoded on pJT6E. All AmtB variants were correctly localized in the membrane fraction (Fig. 1C and data not shown).

**Purification of the AmtB-GlnK Complex**—Purification was carried out using GT1000(pAD2) grown overnight in M9Gln and then subjected to an ammonium shock to deuridylylate GlnK and target it to the membrane (31, 32). The membrane fraction was solubilized in a zwitterionic detergent (LDAO), and the complex was purified after two-step chromatography: Ni<sup>2+</sup> affinity and size exclusion. The complex was also purified

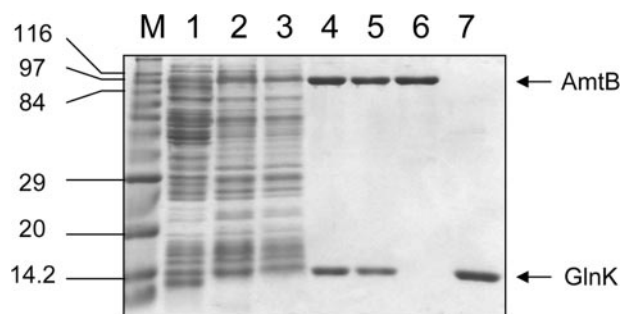


**FIGURE 2. Purification of the AmtB-GlnK complex.** SDS-PAGE (12.5%) showing fractions from the complex purification steps. Lanes 1–7, whole cell extracts (5  $\mu$ g), insoluble membrane fraction (5  $\mu$ g), soluble membrane fraction (3  $\mu$ g), positive fractions pooled after Ni<sup>2+</sup>-column (5  $\mu$ g), positive fractions pooled after S12-column (2.5  $\mu$ g), pure AmtB (2.8  $\mu$ g), and pure GlnK (1  $\mu$ g), respectively. Molecular mass markers (M) in kDa are shown on the left.

and stable in the nonionic detergents *n*-octyl- $\beta$ -D-glucopyranoside and *n*-dodecyl- $\beta$ -D-maltopyranoside (data not shown), but this material was not further characterized.

After the Ni<sup>2+</sup> column, two major bands were obtained on a 12.5% SDS-PAGE gel: the upper band at  $\sim 97$  kDa and the lower one at  $\sim 14$  kDa, masses that match those of pure trimeric AmtB and monomeric GlnK, respectively (Fig. 2). We also confirmed the identities of these proteins as AmtB and GlnK by Western blotting (data not shown). Co-elution of the two proteins after size exclusion chromatography (Fig. 3A) confirms that GlnK does not bind nonspecifically to the Ni<sup>2+</sup> matrix but is complexed with AmtB. Further evidence that GlnK is bound to AmtB is derived from the range of the observed volume for the co-elution of AmtB and GlnK (10.5–12.5 ml) (Fig. 3A), which is distinct from the elution volume of native trimeric GlnK ( $\sim 13.5$  ml) (Fig. 3B). Successful co-purification of GlnK and AmtB without any detectable contaminating proteins confirms a stable and direct interaction between those two proteins (Figs. 2 and 3A). The identity of AmtB and GlnK in the complex was also confirmed by N-terminal sequencing using automated Edman degradation. A single sequence was obtained for GlnK giving MKLVTVI as the first seven residues. Two N-terminal sequences were obtained for AmtB, the major one being APAVAH for the first six residues and the second much more minor sequence being PAVAAH, confirming that maturation of APAVAH<sub>6</sub>-AmtB occurs at the expected cleavage site (1, 4, 5). Interestingly, the protein is not recognized by anti-His tag antibodies (Qiagen) on a Western blot, suggesting that the N-terminal tag is not accessible to the antibodies.

**Status of GlnK in the Complex**—The whole cell extract and the cytosolic fraction from the culture used to purify the complex were analyzed by Western blotting of native polyacrylamide gels using anti-GlnK antibodies. Whole cell extracts of GT1000(pAD6) and GT1000(pAD5) expressing GlnK(Y51F) AmtB and GlnK(WT) AmtB were used as controls for the deuridylylated and the fully uridylylated status, respectively. This revealed that only one form of GlnK was present and that this form ran exactly as deuridylylated GlnK(Y51F) used as control (Fig. 4). To confirm that analysis of whole cell extracts by native PAGE correctly reflects the form of GlnK co-purifying with AmtB, we used mass spectrometry to investigate the status of GlnK that had been dissociated from the purified complex.

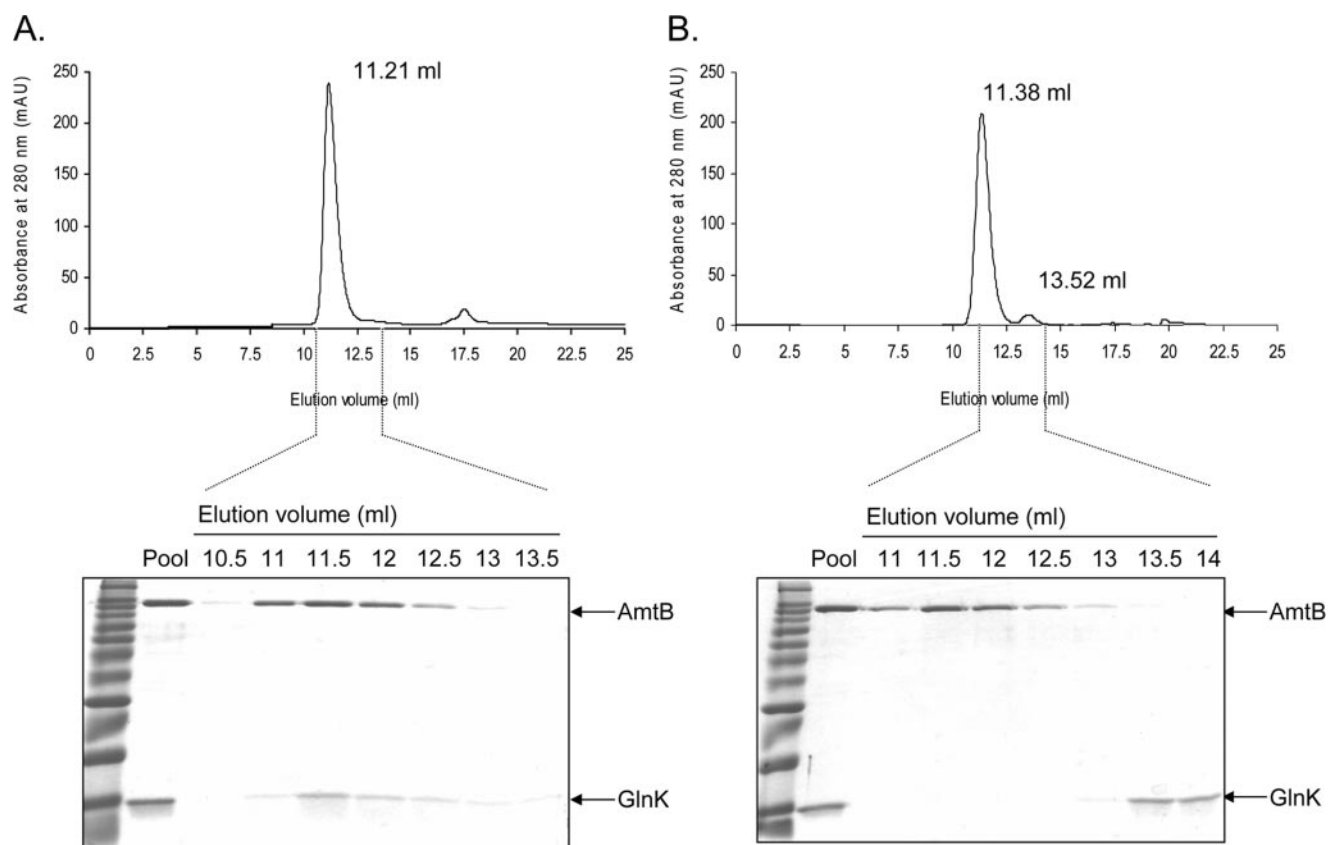


**FIGURE 3. Size exclusion chromatography of the purified complex.** Chromatography was performed on a Superose 12 10/300 GL column using 50 mM Tris-HCl, pH 8.0, 10% (v/v) glycerol, 0.05% (w/v) LDAO, and 100 mM NaCl (A) or 250 mM NaCl (B) as buffer. The elution volumes indicated are an average of four independent runs. The Superose 12 10/300 GL was calibrated with a range of molecular mass standards (Sigma and Amersham Biosciences), and their elution volumes are reported in parentheses:  $\beta$ -amylase, 200 kDa (10.98 ml); aldolase, 158 kDa (11.53 ml); bovine serum albumin, 67 kDa (12.25 ml); carbonic anhydrase, 29 kDa (14.13 ml); cytochrome c, 12.4 kDa (15.22 ml). The injected sample (Pool) and the eluted fractions were analyzed for the presence of AmtB and GlnK on a 12.5% SDS-polyacrylamide gel.

Only one peak was obtained, indicating that only one form of GlnK co-purifies with AmtB. Two independent analyses gave an average mass of  $12,260.53 \pm 2.72$  Da that compares with a mass for purified deuridylylated GlnK of 12,260.69 Da (data not shown) and is in very good agreement with the predicted value of 12,259 Da, assuming an error in the method of 0.01% ( $\pm 1.23$  Da). Hence, we conclude that only the deuridylylated form of GlnK co-purifies with AmtB.

**Size Exclusion Chromatography Analysis of the Complex—**We compared the elution profiles from size exclusion chromatography of the complex with those of free AmtB and free GlnK. In a 100 mM NaCl buffer (Fig. 3A), AmtB and GlnK co-eluted in a single peak at an elution volume of  $11.21 \pm 0.03$  ml ( $n = 4$ ). Calibration of the column showed this to equate to an apparent molecular mass of 153 kDa. However, in the presence of 250 mM NaCl buffer (Fig. 3B), AmtB and GlnK dissociated and eluted in two distinct peaks at  $11.38 \pm 0.03$  ml ( $n = 4$ ) and  $13.52 \pm 0.02$  ml ( $n = 4$ ), respectively. The elution volume of AmtB (11.38 ml) from the complex was very close to the elution volume ( $11.40 \pm 0.02$  ml,  $n = 4$ ) of AmtB purified from GT1000(pAD4), which expresses only AmtB, when run in exactly the same conditions (data not shown). The apparent molecular masses of the proteins dissociated from the complex were calculated to be 137 kDa for AmtB and 34.9 kDa for GlnK,

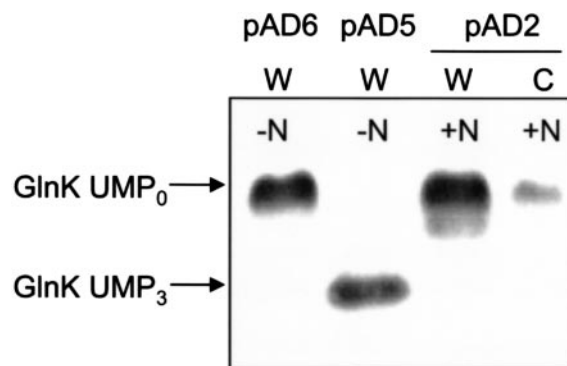


**FIGURE 4. Status of GlnK.** Native PAGE was followed by Western blotting using anti-GlnK antibodies (1:5000). Whole cell extracts (W) of GT1000(pAD6) and GT1000(pAD5) expressing GlnK(Y51F) AmtB and GlnK AmtB, respectively, were used as controls for the deuridylylated and the fully uridylylated status. The whole cell extract and cytoplasmic (C) fraction prepared from GT1000(pAD2) expressing GlnK AP(AVAH)<sub>6</sub>-AmtB were analyzed. Cells were harvested before (-N) or after an ammonium shock (+N).

which are close to the expected values of 130 and 36.8 kDa, respectively.

**Stoichiometry of the Complex—**We investigated the stoichiometry of the AmtB-GlnK complex by two approaches: first using the amino acid composition and second using titration on gels revealed by Coomassie Blue staining. The AmtB/GlnK stoi-

## *E. coli* AmtB-GlnK Complex

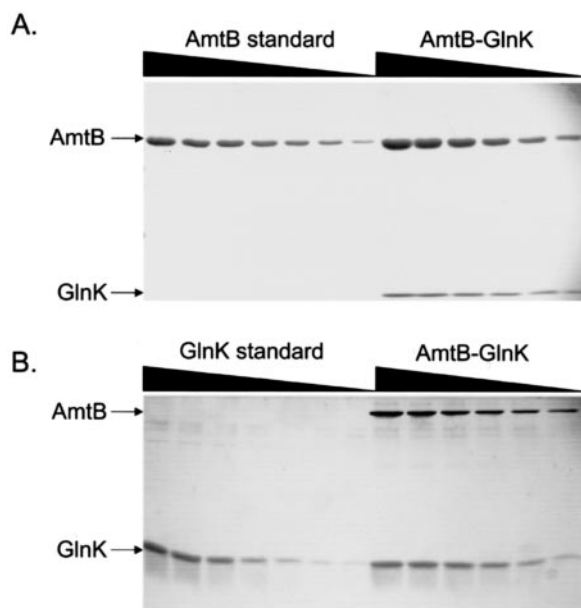


FIGURE 5. **Quantitation of AmtB/GlnK stoichiometry by SDS-PAGE.** Each gel contains a standard curve for the protein and dilutions of the complex for quantitation as described under "Experimental Procedures." *A*, AmtB (10% SDS-PAGE); *B*, GlnK (15% SDS-PAGE).

chometry calculated from the amino acid composition of the purified complex was 1:1.1 (see supplemental Table S1). As explained under "Experimental Procedures," this value was calculated using the data obtained for all of the amino acids detected by the method except for Val and Ile. The stoichiometry calculated using quantitative Coomassie gels was also 1:1.1  $\pm$  0.2 ( $n = 4$ ) (Fig. 5), using four values that fell within the standard curves (bearing in mind that AmtB runs as a trimer and GlnK as a monomer on SDS-PAGE). Hence, both methods gave an AmtB/GlnK stoichiometry of 1:1, indicating that after purification of the complex, in the presence of detergent, AmtB and GlnK are equimolar.

**In Vitro Influence of Small Effectors on the AmtB-GlnK Complex**—The successful purification of the complex allowed us to study the *in vitro* requirements for dissociation and association of the component proteins. Efficient dissociation of GlnK, as deduced by its presence in the 5 mM imidazole wash fractions (Wash 1 and 2), required 2-OG (1 or 2 mM), ATP (3.5 mM), and MgCl<sub>2</sub> (5 mM) together (Fig. 6, *A* and *B*, lanes 4 and 5, and supplemental Table S2). Dissociation was also observed in the control conditions using 0.6 M NaCl (Fig. 6, *A* and *B*, lane 2, and supplemental Table S2). However, when the 2-OG concentration was reduced to 0.1 mM, with ATP and MgCl<sub>2</sub> unchanged, the majority of GlnK coeluted with AmtB (Fig. 6, *A* and *B*, lane 3, and supplemental Table S2). Sensitivity of dissociation to the 2-OG concentration was only observed in the presence of both MgCl<sub>2</sub> and ATP. However, significant dissociation was also observed in the presence of MgCl<sub>2</sub> with or without 2-OG (0.1 and 2 mM) (Fig. 6, *A* and *B*, lanes 9, 11, and 13, and supplemental Table S2).

The complex was stable in the absence of effectors, in the presence of ATP alone, or when ATP was present with either 2-OG or MgCl<sub>2</sub> (Fig. 6, *A* and *B*, lanes 1, 8, 10, 12, and 14, and supplemental Table S2). Likewise, when only 2-OG was added,

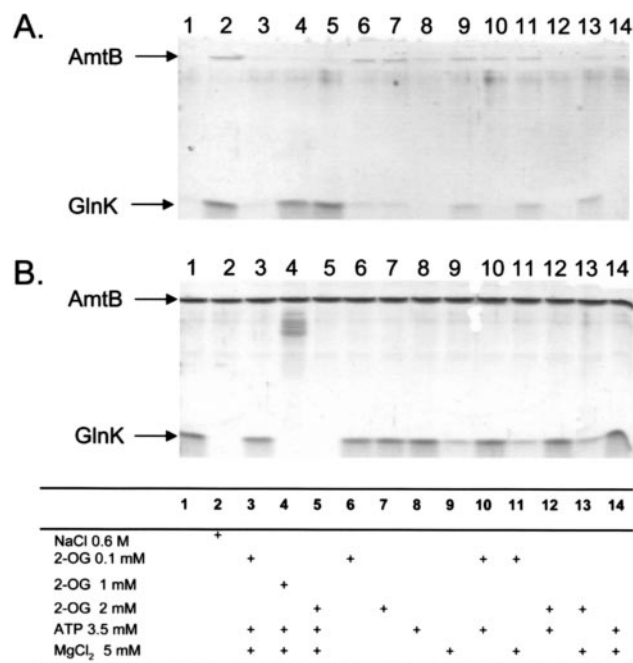


FIGURE 6. **Effect of small effectors on stability of the AmtB-GlnK complex.** 12.5% SDS-PAGE of the Wash 1 fraction collected in the absence or presence of small effectors (*A*) and the eluted fraction (*B*). The Wash 2 fraction was also analyzed by SDS-PAGE, and in most fractions some GlnK was still present (see supplemental Table S2). The table at the bottom reports the composition of the buffers applied to the column after immobilization of the purified complex on the Ni<sup>2+</sup> matrix. Gels were stained with Coomassie Blue.

the majority of GlnK still coeluted with AmtB, irrespective of the 2-OG concentration (Fig. 6*A*, lanes 6 and 7, and supplemental Table S2).

To examine the conditions required to reconstitute the AmtB-GlnK complex *in vitro*, we used exactly the same combinations of effectors as those used for dissociation, except that the control condition in the presence of 0.6 M NaCl (lane 2 for the dissociation experiment) was not included. GlnK coeluted with AmtB in the presence of MgCl<sub>2</sub> (5 mM), ATP (3.5 mM), and 2-OG (0.1 mM) (Fig. 7*B*, lane 3). However, in the same conditions, if the 2-OG concentration was  $\geq$  1 mM, GlnK did not associate with AmtB (Fig. 7*B*, lanes 4 and 5). Interestingly, higher amounts of GlnK were coeluted with AmtB in the presence of ATP with or without 2-OG (0.1 or 2 mM) or MgCl<sub>2</sub> (Fig. 7*B*, lanes 8, 10, 12, and 14). The amount of AmtB present in the eluted fraction was similar for all of the conditions tested (Fig. 7*A*); therefore, the different amounts of GlnK eluted are specific for the effectors added. Furthermore, we confirmed that binding of GlnK was specific to AmtB, because in the absence of AmtB no GlnK was eluted (data not shown).

## DISCUSSION

The co-purification of GlnK with AmtB from ammonium-shocked *E. coli* cells definitively demonstrates that these two proteins form a functional complex with a stoichiometry of 1:1. No other protein component is closely associated with the complex, although we cannot exclude the possibility that *in vivo* there could be circumstances where other less tightly bound proteins could also interact. In addition to the GlnK-NifA, GlnK-NifL, and GlnK-NifA-NifL complexes (38), the AmtB-

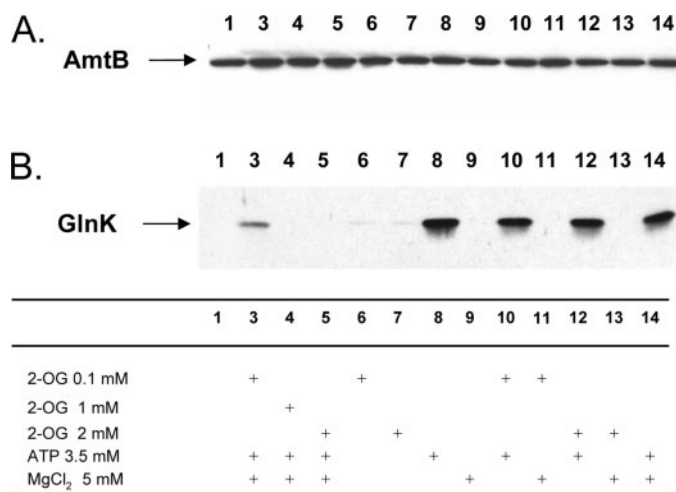


FIGURE 7. *In vitro* reconstitution of the AmtB-GlnK complex. Reactions were as described under "Experimental Procedures." The eluted fraction was analyzed by Western blot for the presence of AmtB (A) and GlnK (B). The table at the bottom reports the composition of the buffers used to preincubate the AmtB and GlnK mixture, which are identical to those used in Fig. 6, except that the control condition (lane 2 in Fig. 6) was not repeated in this set of experiments.

GlnK complex is the second reported complex involving a P<sub>II</sub> protein to be purified from *in vivo* extracts, all other studies having involved *in vitro* reconstitution of the P<sub>II</sub>-receptor complexes. P<sub>II</sub> proteins are known to interact with a wide variety of target proteins and thereby regulate many facets of nitrogen metabolism, but to date, relatively few P<sub>II</sub> complexes have been studied in detail. In *Synechococcus elongatus*, the P<sub>II</sub> protein forms a complex with a key enzyme in arginine biosynthesis, *N*-acetyl-L-glutamate kinase (39), and *in vitro* reconstitution of this complex showed a 1:1 stoichiometry in which a single P<sub>II</sub> trimer binds a single *N*-acetyl-L-glutamate kinase hexamer (40). The same stoichiometry was recently reported for the P<sub>II</sub>-*N*-acetyl-L-glutamate kinase complex from *Arabidopsis thaliana* (41). The stoichiometry of one other binary complex involving P<sub>II</sub> has been reported in *Methanosarcina mazei*, where two molecules of trimeric GlnK were proposed to bind to one dodecamer of glutamine synthetase (42).

To date, the detailed binding mode of any P<sub>II</sub> protein with its target has not been reported, although direct involvement of the T-loop in the interaction has been shown for GlnD-P<sub>II</sub> complexes (20, 21) and also for the GlnB-NtrB complex (23). Consistent with these ideas, the T-loops have also been proposed to play an important role in the AmtB-GlnK interaction (7). In a docking model of a hypothetical complex of *A. fulgidus* Amt-1 and GlnB-1, the authors suggest that the GlnB-1 T-loops could insert deeply into the cytoplasmic ends of the substrate channels of Amt-1 (7). Crystal structures of a number of P<sub>II</sub> proteins suggest that the T-loop is highly flexible and can adopt a variety of conformations. Furthermore, the location of the uridylylation site (Tyr-51) at the apex of the T-loop means that uridylylation will significantly change this surface of the protein. In this regard, it is notable that only fully deuridylylated GlnK is present in the purified AmtB-GlnK complex, suggesting that uridylylation of just a single T-loop may be incompatible with complex formation. However, we cannot rule out that other forms of GlnK could also be present *in vivo* and only loosely bound, so

that they are lost during the purification process. GlnK must interact with the cytoplasmic face of AmtB, and we have shown previously that deletion of the C-terminal cytoplasmic region of AmtB prevents GlnK association (32). The docking model for *A. fulgidus* Amt-1 and GlnB-1 also concludes that residues in the C-terminal region of Amt-1 are likely to be important for GlnB-1 interaction (7).

Our data show that the complex stability is sensitive to 250 mM NaCl. Therefore, electrostatic interactions could be involved in the interaction between GlnK and AmtB. The addition of salts could also affect the interaction between GlnK and noncovalently bound effectors, as discussed later, thereby affecting the conformation of the protein. Hydrophobic interactions do not appear to be of major importance, because the complex is not dissociated after solubilization and purification in nonionic (*n*-octyl- $\beta$ -D-glucopyranoside and *n*-dodecyl- $\beta$ -D-maltopyranoside) and zwitterionic (LDAO) detergents. These observations are in agreement with the proposed docking model between *A. fulgidus* Amt-1 and GlnB-1, where it was argued that the negative electrostatic surface potential of GlnB-1 matches the slightly positively charged cytoplasmic face of Amt-1 (7). However, whereas *E. coli* AmtB also has a positive net charge on its cytoplasmic face (5), the net surface charge of *E. coli* GlnK, as it occurs in the complex, cannot realistically be calculated, because we do not know the status of small effectors, such as 2-OG and ATP.

Biochemical studies have established that binding of ATP and 2-OG to P<sub>II</sub> proteins influences interactions with their receptors. Although the factors affecting formation of P<sub>II</sub>-receptor complexes have been described in a few cases, factors affecting dissociation have only been reported for the *S. elongatus* P<sub>II</sub>-*N*-acetyl-L-glutamate kinase complex (40). We have studied the roles of these effectors *in vitro* in both formation and dissociation of the AmtB-GlnK complex. We find that the AmtB-GlnK interaction is sensitive to ATP, Mg<sup>2+</sup>, and 2-OG *in vitro*, and consequently, deuridylylated GlnK is not able to bind to AmtB in the absence of effectors.

Complex formation occurs efficiently in the presence of ATP alone. We believe that this effect is likely to be mediated via the known interaction of ATP with GlnK (16), although we cannot formally exclude an interaction of ATP with AmtB. *E. coli* GlnK and GlnB have three ATP-binding sites located in the lateral clefts between the subunits (16, 43), and it has been suggested that ATP binding could affect the structure and mobility of the T-loop (16). Consistent with this, our data suggest that ATP binding to GlnK could induce a change of its conformation, enabling the interaction with AmtB, and, as discussed earlier, the T-loop of GlnK seems likely to be involved in that interaction.

GlnK binding to AmtB is also observed in the presence of ATP, 0.1 mM 2-OG, and MgCl<sub>2</sub>, although this binding is notably weaker than in the presence of ATP alone or ATP with either 2-OG (0.1 or 2 mM) or MgCl<sub>2</sub>. As with ATP, we cannot presently exclude the possibility that 2-OG acts by binding directly to AmtB, but it seems more likely to mediate its effects through GlnK. For *E. coli* GlnB, the binding of ATP and 2-OG is synergistic (27). Such properties could explain the observed ATP dependence of the 2-OG effects on the complex.

## *E. coli* AmtB-GlnK Complex

The apparent interactive effects of the two effectors could reflect the fact that their binding sites are close to each other. No crystal structure is yet available for 2-OG bound to a P<sub>II</sub> protein. However, based on structural comparisons of *Herbaspirillum seropedicae* GlnB with other  $\alpha$ -keto acid-binding proteins, the 2-OG binding site has been proposed to be in the cleft and in the vicinity of the  $\gamma$ -phosphate of ATP (44). This suggestion is also supported by biochemical data from dephosphorylation studies of cyanobacterial GlnB (45). Furthermore, two different binding modes of ATP have been reported for *E. coli* GlnB (43), and one of these could represent a 2-OG-bound state.

In the presence of ATP and MgCl<sub>2</sub>, the complex is sensitive to 2-OG, such that an increase in 2-OG concentration from 0.1 to 1 mM dissociates the complex. Effects of 2-OG concentration on the formation of a P<sub>II</sub>-receptor complex have been described for the *S. elongatus* P<sub>II</sub>-N-acetyl-L-glutamate kinase complex (40), the *A. vinelandii* GlnK-NifL complex (46), and the interactions of *E. coli* GlnB and GlnK with their targets (21, 27–30).

It was reported that *E. coli* GlnB (24, 27) (and suggested that *E. coli* GlnK (21)) binds one molecule of 2-OG with high affinity and that up to three molecules could be bound, leading to an altered conformation. Such a change of conformation could potentially promote dissociation of the AmtB-GlnK complex, as proposed for the interaction of GlnK with NtrB or GlnE (21). So far in *E. coli*, the intracellular 2-OG level has been reported to fluctuate between 0.1 and 0.9 mM (47) in cells grown in a glucose-limited chemostat with an ammonium excess. However, the 2-OG levels in different nitrogen conditions have not yet been examined in *E. coli*, and the possible physiological significance of the effects of 2-OG on the AmtB-GlnK complex remains to be investigated.

Finally, our *in vitro* studies indicate that the sensitivity to 2-OG of the AmtB-GlnK complex is only apparent when MgCl<sub>2</sub> and ATP are both present. A putative 2-OG-binding site in the close vicinity of the ATP site, as discussed earlier, constitutes a potential problem in accommodating the proximity of the negative charges of the ATP phosphate groups and the carboxyl groups of 2-OG. The presence of Mg<sup>2+</sup> could serve to balance these negative charges, thereby allowing the binding of 2-OG in the close vicinity of ATP, as suggested by Xu *et al.* (16) and as also observed for the oxalate-ATP complex with pyruvate kinase (48).

Altogether, our data suggest that the AmtB-GlnK interaction might not be exclusively regulated *in vivo* by uridylylation but that it could also be affected by ATP and 2-OG, although the physiological relevance of these effectors has yet to be elucidated.

The precise physiological role of the AmtB-GlnK interaction remains to be determined, although current data support the idea that binding of GlnK to AmtB inhibits the activity of the channel (31, 32). In discussing their Amt-1-GlnB-1 complex model, Andrade *et al.* suggest that the T-loops of the P<sub>II</sub> protein could inactivate the Amt protein by simple steric blocking of the substrate channels (7). Alternatively, Zheng *et al.* considered a model in which AmtB can adopt at least two conformational states, one of which is a nonconducting state, and this closed conformation might be induced by binding of GlnK (6).

In this context, it is interesting to note that in *B. subtilis*, GlnK (NrgB) is apparently bound to AmtB (NrgA) even under nitrogen-limiting growth conditions, and the activity of AmtB is not impaired (33). Further *in vivo* studies in a variety of organisms are therefore required to elucidate the precise function of GlnK binding to AmtB. Sequestration of GlnK by AmtB also has the potential to facilitate rapid control of other facets of nitrogen metabolism by targeting other cytosolic P<sub>II</sub> partners to the membrane and thereby inactivating them. Such a process has recently been suggested for the control of ADP-ribosylation of nitrogenase in *A. brasilense*, where the GlnK orthologue GlnZ targets DraG (dinitrogenase reductase activating glycohydrolase) to the cell membrane in an AmtB-dependent manner (35).<sup>3</sup>

*Acknowledgments*—We thank Mike Weldon (Department of Biochemistry, University of Cambridge) and Arthur Moir (Krebs Institute Sequencing and Synthesis Facility, University of Sheffield) for N-terminal sequencing and Peter Sharatt (Department of Biochemistry, University of Cambridge) for amino acid composition analysis. Mass spectrometric analysis was carried out by Karen Wilson, Andrew Bottrill, and Mike Naldrett of the Joint IFR-JIC Proteomics Facility. We thank Arnaud Javelle and Emmanuele Severi for construction of plasmids pAJ1023 and pESV4E, pJT6E, pMODULES3, and pSTUART, respectively, and Stephen Bornemann for very helpful advice regarding the stoichiometry calculations. We thank Ray Dixon, Xiao-Dan Li, Elizabeth Scanlon, Alexandre Decors, and Per Bullough for helpful comments on the manuscript.

## REFERENCES

1. von Wirén, N., and Merrick, M. (2004) *Trends Curr. Genet.* **9**, 95–120
2. Blakey, D., Leech, A., Thomas, G. H., Coutts, G., Findlay, K., and Merrick, M. (2002) *Biochem. J.* **364**, 527–535
3. Conroy, M. J., Jamieson, S. J., Blakey, D., Kaufmann, T., Engel, A., Fotiadis, D., Merrick, M., and Bullough, P. A. (2004) *EMBO Rep.* **5**, 1153–1158
4. Thornton, J., Blakey, D., Scanlon, E., and Merrick, M. (2006) *FEMS Microbiol. Lett.* **258**, 114–120
5. Khademi, S., O'Connell, J., III, Remis, J., Robles-Colmenares, Y., Miercke, L. J., and Stroud, R. M. (2004) *Science* **305**, 1587–1594
6. Zheng, L., Kostrewa, D., Bernèche, S., Winkler, F. K., and Li, X.-D. (2004) *Proc. Natl. Acad. Sci. U. S. A.* **101**, 17090–17095
7. Andrade, S. L., Dickmanns, A., Ficner, R., and Einsle, O. (2005) *Proc. Natl. Acad. Sci. U. S. A.* **102**, 14994–14999
8. Liu, Y., and Hu, X. (2006) *J. Phys. Chem. A Mol. Spectrosc. Kinet. Environ. Gen. Theory* **110**, 1375–1381
9. Javelle, A., Thomas, G., Marini, A. M., Kramer, R., and Merrick, M. (2005) *Biochem. J.* **390**, 215–222
10. Winkler, F. K. (2006) *Pflugers Arch.* **451**, 701–707
11. Soupene, E., He, L., Yan, D., and Kustu, S. (1998) *Proc. Natl. Acad. Sci. U. S. A.* **95**, 7030–7034
12. Thomas, G., Coutts, G., and Merrick, M. (2000) *Trends Genet.* **16**, 11–14
13. Arcondéguy, T., Jack, R., and Merrick, M. (2001) *Microbiol. Mol. Biol. Rev.* **65**, 80–105
14. Ninfa, A. J., and Jiang, P. (2005) *Curr. Opin. Microbiol.* **8**, 168–173
15. Forchhammer, K. (2004) *FEMS Microbiol. Rev.* **28**, 319–333
16. Xu, Y., Cheah, E., Carr, P. D., van Heeswijk, W. C., Westerhoff, H. V., Vasudevan, S. G., and Ollis, D. L. (1998) *J. Mol. Biol.* **282**, 149–165
17. Cheah, E., Carr, P. D., Suffolk, P. M., Vasudevan, S. G., Dixon, N. E., and Ollis, D. L. (1994) *Structure* **2**, 981–990

<sup>3</sup> Huergo, L. F., Chubatsu, L. S., Souza, E. M., Pedrosa, F. O., Steffens, M. B. R., and Merrick, M. (2006) *FEBS Lett.*, in press.

18. Carr, P. D., Cheah, E., Suffolk, P. M., Vasudevan, S. G., Dixon, N. E., and Ollis, D. L. (1996) *Acta Crystallogr. Sect. D* **52**, 93–104
19. Jiang, P., Zucker, P., Atkinson, M. R., Kamberov, E. S., Tirasophon, W., Chandran, P., Scheffe, B. R., and Ninfa, A. J. (1997) *J. Bacteriol.* **179**, 4342–4353
20. Jaggi, R., Ybarlucea, W., Cheah, E., Carr, P. D., Edwards, K. J., Ollis, D., and Vasudevan, S. G. (1996) *FEBS Lett.* **391**, 223–228
21. Atkinson, M., and Ninfa, A. J. (1999) *Mol. Microbiol.* **32**, 301–313
22. Martinez-Argudo, I., and Contreras, A. (2002) *J. Bacteriol.* **184**, 3746–3748
23. Pioszak, A. A., Jiang, P., and Ninfa, A. J. (2000) *Biochemistry* **39**, 13450–13461
24. Jiang, P., Peliska, J. A., and Ninfa, A. J. (1998) *Biochemistry* **37**, 12782–12794
25. Son, H. S., and Rhee, S. G. (1987) *J. Biol. Chem.* **262**, 8690–8695
26. van Heeswijk, W. C., Hoving, S., Molenaar, D., Stegeman, B., Kahn, D., and Westerhoff, H. V. (1996) *Mol. Microbiol.* **21**, 133–146
27. Kamberov, E. S., Atkinson, M. R., and Ninfa, A. J. (1995) *J. Biol. Chem.* **270**, 17797–17807
28. Jiang, P., and Ninfa, A. J. (1999) *J. Bacteriol.* **181**, 1906–1911
29. Jiang, P., Peliska, J. A., and Ninfa, A. J. (1998) *Biochemistry* **37**, 12795–12801
30. Jiang, P., Peliska, J. A., and Ninfa, A. J. (1998) *Biochemistry* **37**, 12802–12810
31. Javelle, A., Severi, E., Thornton, J., and Merrick, M. (2004) *J. Biol. Chem.* **279**, 8530–8538
32. Coutts, G., Thomas, G., Blakey, D., and Merrick, M. (2002) *EMBO J.* **21**, 536–545
33. Detsch, C., and Stulke, J. (2003) *Microbiology* **149**, 3289–3297
34. Strosser, J., Ludke, A., Schaffer, S., Kramer, R., and Burkovski, A. (2004) *Mol. Microbiol.* **54**, 132–147
35. Huergo, L. F., Souza, E. M., Araujo, M. S., Pedrosa, F. O., Chubatsu, L. S., Steffens, M. B., and Merrick, M. (2006) *Mol. Microbiol.* **59**, 326–337
36. Javelle, A., and Merrick, M. (2005) *Biochem. Soc. Trans.* **33**, 174–176
37. Spackman, D., Stein, W., and Moore, S. (1958) *Anal. Chem.* **30**, 1190–1206
38. Stips, J., Thummer, R., Neumann, M., and Schmitz, R. A. (2004) *Eur. J. Biochem.* **271**, 3379–3388
39. Heinrich, A., Maheswaran, M., Ruppert, U., and Forchhammer, K. (2004) *Mol. Microbiol.* **52**, 1303–1314
40. Maheswaran, M., Urbanke, C., and Forchhammer, K. (2004) *J. Biol. Chem.* **279**, 55202–55210
41. Chen, Y. M., Ferrar, T. S., Lohmeir-Vogel, E., Morrice, N., Mizuno, Y., Berenger, B., Ng, K. K., Muench, D. G., and Moorhead, G. B. (2006) *J. Biol. Chem.* **281**, 5726–5733
42. Ehlers, C., Weidenbach, K., Veit, K., Forchhammer, K., and Schmitz, R. A. (2005) *Mol. Microbiol.* **55**, 1841–1854
43. Xu, Y., Carr, P. D., Huber, T., Vasudevan, S. G., and Ollis, D. L. (2001) *Eur. J. Biochem.* **268**, 2028–2037
44. Benelli, E. M., Buck, M., Polikarpov, I., de Souza, E. M., Cruz, L. M., and Pedrosa, F. O. (2002) *Eur. J. Biochem.* **269**, 3296–3303
45. Ruppert, U., Irmmler, A., Kloft, N., and Forchhammer, K. (2002) *Mol. Microbiol.* **44**, 855–864
46. Little, R., Colombo, V., Leech, A., and Dixon, R. (2002) *J. Biol. Chem.* **277**, 15472–15481
47. Senior, P. J. (1975) *J. Bacteriol.* **123**, 407–418
48. Lodato, D. T., and Reed, G. H. (1987) *Biochemistry* **26**, 2243–2250